

---

# MACHINE LEARNING FOR OPTICAL MOTION CAPTURE-DRIVEN MUSCULOSKELETAL MODELING FROM INERTIAL MOTION CAPTURE DATA

---

\*

**Abhishek Dasgupta** 

Doctoral Training Centre,  
1–4 Keble Road,  
University of Oxford,  
Oxford OX1 3NP, United Kingdom;  
abhishek.dasgupta@dtc.ox.ac.uk

**Rahul Sharma** 

Laboratory for Computation and Visualization  
in Mathematics and Mechanics,  
Institute of Mathematics,  
École Polytechnique Fédérale de Lausanne,  
Lausanne 1015, Switzerland;  
rahul.sharma@epfl.ch

**Challenger Mishra** 

Department of Computer Science & Technology,  
University of Cambridge,  
15 J.J. Thomson Ave.,  
Cambridge CB3 0FD, United Kingdom;  
cm2099@cam.ac.uk

**Vikranth H. Nagaraja** 

Department of Engineering Science,  
Institute of Biomedical Engineering,  
University of Oxford,  
Old Road Campus Research Building,  
Oxford OX3 7DQ, United Kingdom;  
vikranth.harthikotenagaraja@eng.ox.ac.uk

## ABSTRACT

Marker-based Optical Motion Capture (OMC) systems and the associated musculoskeletal (MSK) modeling predictions have offered the ability to gain insights into *in vivo* joint and muscle loading non-invasively as well as aid clinical decision-making. However, an OMC system is lab-based, expensive, and requires a line of sight. A widely used alternative is the Inertial Motion Capture (IMC) system, which is portable, user-friendly, and relatively low cost, although it is not as accurate as an OMC system. Irrespective of the choice of motion capture technique, one needs to use an MSK model to obtain the kinematic and kinetic outputs, which is a computationally expensive tool increasingly well approximated by machine learning (ML) methods. Here, we present an ML approach to map IMC data to the human upper-extremity MSK outputs computed from OMC input data. Essentially, we attempt to predict high-quality MSK outputs from the relatively easier-to-obtain IMC data. We use OMC and IMC data simultaneously collected for the same subjects to train an ML (feed-forward multi-layer perceptron) model that predicts OMC-based MSK outputs from IMC measurements. We demonstrate that our ML predictions have a high degree of agreement with the desired OMC-based MSK estimates. Thus, this approach will be instrumental in getting the technology from ‘lab to field’ where OMC-based systems are infeasible.

**Keywords** Inertial Motion Capture · Machine learning · Musculoskeletal modeling · Neural network · Optical Motion Capture · Prediction · Upper Extremity

---

\**Citation:* Dasgupta, A., Sharma, R., Mishra, C., and Nagaraja, V.H. Machine Learning for Optical Motion Capture-driven Musculoskeletal Modeling from Inertial Motion Capture Data. 2022. 1–19.

## 1 Introduction

Three-dimensional (3D) motion analysis helps numerically describe joint and segmental kinematics. Besides, it serves to establish non-disabled and identify pathological movement patterns [1, 2]. In recent decades, *in silico* musculoskeletal (MSK) models have offered the ability to non-invasively estimate information to facilitate objective, clinical decision-making to some extent [3, 4, 5, 6]. In particular, the prediction of intersegmental/joint and muscle loading has proven to be immensely valuable in improving our understanding of the MSK system [3]. However, traditional MSK models can be computationally expensive and typically require extensive input motion capture (mocap) data [3, 7]. In addition, current MSK models can be laborious and too time-consuming to create, scale, and set up for individual subjects. Furthermore, licenses for commercial MSK modeling software can be prohibitively expensive, and some of the open-source packages might be limiting concerning applications and/or features. Thus, computational complexity and implementation difficulties prohibit the routine use of this technique in clinical settings and restrict its use to research environments [3]. Consequently, despite the ability to assess *in vivo* joint and muscle loading information during a functional activity of interest, there is little evidence showing the use of MSK modeling for clinical treatment planning, especially in the upper extremity [7, 8].

A plethora of research and commercial mocap systems help capture 3D human movement data accurately and repeatably [9] that can subsequently help describe the MSK function. Nonetheless, each motion tracking method is accompanied by its pros and cons [9, 2, 10]. Anglin and Wyss [2] noted that stereophotogrammetric (or optoelectronic) systems with passive retro-reflective markers seem particularly suited for upper-extremity motion analysis [11] since they are non-invasive, have high accuracy, and generally do not influence task execution. However, the primary drawbacks of a marker-based Optical Motion Capture (OMC) system include marker occlusion (i.e., line-of-sight requirement), high cost, being lab-based, etc. Conversely, an Inertial Motion Capture (IMC) system is relatively portable and cost-effective, user-friendly, and provides full-body measurement capabilities in the subject's ecological setting or 'field condition.' However, IMC systems might not be as accurate as OMC systems, which are widely regarded as the 'gold standard' for non-invasive mocap. Regardless, this 'field ready' option of IMC systems can be immensely valuable in low-resource settings as well as outdoor/real-world applications (e.g., sports, ergonomics). Wearable inertial sensors have evolved rapidly and are routinely used in different areas of clinical human movement analysis, e.g., gait analysis [12], stabilometry, instrumented clinical tests, upper-extremity mobility assessment, daily-life activity monitoring, and tremor assessment [13]. A recent review also opined that inertial measurement unit (IMU)-based wearable devices have undergone a rapid transition from use in laboratory-based clinical practice to unsupervised, applied settings [14]. Inverse-dynamics-based MSK models have traditionally been driven by OMC data [15, 16]), however, recent studies have demonstrated the use of IMC input for MSK models [17, 18, 19, 20, 21, 22, 23].

There is a growing need to democratize and take objective MSK model-based analysis from 'lab to field' [24, 25], and this field has started gaining attention in the recent past. Notwithstanding, research on upper-extremity biomechanics has lagged compared to that involving the lower extremity [1, 2, 26] due to several barriers such as a lack of consensus on a standardized protocol, functional tasks, model complexity, tracking method, marker protocol, and performance metrics. It is imperative to undertake better modeling of upper-extremity biomechanics as they are integral to many activities of daily living.

In this direction, machine learning (ML) can play a substantial role and has received much attention in human motion analysis, especially in the last decade [27, 25, 28]. In particular, the use of supervised ML models to bypass computationally expensive optimization problems has become commonplace, ranging from the estimation of deformable joint contact [29] and implant pressure distribution [30] to the estimation of ground reaction forces [31, 32], joint moments [33], and joint forces [34]. Numerous other studies have also reported ML applications for estimating *in vivo* joint and muscle loading information from either OMC or IMC data [35, 36, 37, 38, 39, 31, 40, 41, 42, 43, 44, 34, 45, 32], essentially bypassing the need for an MSK model. Among ML approaches, deep learning models, including Convolutional Neural Networks (CNN) and, increasingly, Recurrent Neural Networks (RNN), are popular, accounting for most ML techniques adopted in lower-extremity biomechanical analyses involving ML [28]. Such ML methods have multiple advantages over their MSK model-based counterparts – (i) while the initial training of the ML model takes time, prediction corresponding to new data is highly efficient; and (ii) they do not require the large amounts of data that are required for MSK models and help provide population-level insights [40]. The use of supervised ML methods also ensures flexibility and informs about population-level relationships (e.g., in product design or ergonomics), in contrast to methods based on independent trials, such as traditional inverse dynamics or kinematics analysis. The efficiency of the ML models also facilitates its use in real-time applications where efficiency is a priority, e.g., in clinical or outdoor settings.

Our previous work [36] estimated upper-extremity MSK model information solely from IMC input data. This study uses ML methods to map IMC input data to OMC-driven MSK outputs. It serves two purposes: (a) bypasses the dependency on the MSK model during the prediction phase, which is advantageous because of the computational inefficiency of

MSK models; and (b) more importantly, obviates the requirement for an OMC system in the prediction phase but still estimates ‘OMC-quality’ MSK outputs. It makes it possible to predict (non-invasive) gold-standard OMC-quality MSK outputs for mobile/ambulatory applications (e.g., sports, recreational activities) or in low-resource settings using highly portable IMC systems. Estimating the ‘gold standard’ OMC-driven MSK outputs from simulated IMU inputs was done in [46] for the lower extremity. This work differs in using actual IMU inputs, which were synchronously collected with the OMC inputs, giving greater reliability in predicting OMC quality outputs and in its application to the upper extremity. Like that study, we have realized our objective using NNs. In particular, we used feed-forward NNs to model the human upper-extremity motion analysis. It is important to note that such a model creation was possible because of the unique dataset acquired in [20], where the upper-extremity motion for five non-disabled subjects was synchronously captured using both IMC and OMC systems. To the best of our knowledge, this is the first study across upper and lower extremities that uses the comparatively lower-quality (but highly portable) IMC data to estimate kinematic and kinetic variables on par with the gold standard OMC-driven MSK outputs. Such an approach will be instrumental in getting the technology from ‘lab to field’ where OMC-based systems are infeasible.

Finally, along with an entirely novel approach to map IMC inputs to OMC-driven MSK outputs, this study also addresses several other research gaps in this field. For instance, most research in this field lacks rigorous hyperparameter tuning when training ML architectures (highlighted in [27] and [36]) which is crucial for generalizable models. Moreover, we trained the ML model for two different settings – subject-naive (all trials from a subject are strictly either in test or training data) and subject-exposed (at least one trial from each subject is used in the training of the model). The subject-naive setting is the true check for the generalizability of the ML model, which is often ignored. Moreover, from the motion analysis point of view, this study focuses on modeling the human upper extremity (an under-represented but essential domain), and the ML model allows us to estimate the relevant kinematic and kinetic MSK parameters.

## 2 Materials and methods

### 2.1 Data

The anonymized dataset used here is from an earlier study [20], approved by local Research Ethics Committees (Ref no. 16/SC/0051 and Ref no. 14/LO/1975). The study involved five male adult non-disabled volunteers (Age:  $22.80 \pm 0.84$  years; Height:  $1.75 \pm 0.07$  m; Weight:  $66.25 \pm 9.72$  kg; Body Mass Index (BMI):  $21.79 \pm 3.49$  kg/m<sup>2</sup>) had consented to participate.

For each subject, three trials of the Reach-to-Grasp task in the *Forward* direction were executed at a self-selected pace using a custom-built apparatus (Supplementary Figure 1) to adjust the anthropometric requirements of different participants and facilitate the execution of the *Reach-to-Grasp* task in a seated position. The task involved the participant reaching to grasp a ‘dumbbell-shaped’ object and moving it between various pre-defined points as instructed. The pre-defined ‘*Front*’ point was within 90% of an individual’s arm length (i.e., acromion to middle-fingertip length, with the arm hanging down) to minimize the contribution of trunk movement for task execution [47, 48].

Synchronized data capture corresponding to task execution involved a 16-camera Vicon™ T40S Series System (Vicon Motion Systems, Oxford, UK) for OMC input data (sampling frequency: 100 Hz) and a Full-body Xsens MVN Awinda Station with 17 wireless IMU sensors (Xsens Technologies B. V., Enschede, The Netherlands) for the IMC input data (sampling frequency: 60 Hz). Passive retro-reflective markers ( $\varnothing$  9.5 mm) were placed on the participant’s skin using a double-sided hypoallergenic tape using the Plug-in Gait marker set [49]. Each IMU contains a 3D accelerometer, gyroscope and magnetometer, along with a barometer and thermometer, and transmits data wirelessly to a master receiver in real-time [50]. IMU sensors placement on the participants’ body segments and their setup and calibration were based on the recommended protocol from the Xsens MVN User Manual [51]. Data capture was synchronized between the two systems wherein the Xsens IMC system triggered the Vicon OMC system following the guidelines of Xsens with a specific trigger at the start/stop recording time [52]. Marker and sensor placement, as well as data capture for all subjects, were performed by the same tester (VHN) to remove inter-tester variability error.

OMC data was processed using Vicon Nexus™ v.2.5 software [53] to clean and label the marker trajectories for MSK model inputs. The processed marker trajectories were exported in Coordinate 3D (.C3D) file format [54]. Meanwhile, the affiliated Xsens MVN Analyze 2018 software [55] was used to capture the IMC data and export it as BioVision Hierarchy (.BVH) files for MSK model inputs where a stick-figure model was initially reconstructed. Upper-extremity MSK modeling was carried out using AnyBody™ Modeling System (AnyBody™ Technology A/S, Aalborg, Denmark) separately for each of the mocap inputs as well as subject-specific anthropometric dimensions for scaling following these sources [56, 17]. The ‘*Simple Full-Body model*’ and ‘*Inertial MoCap model*’ in the AnyBody Managed Model Repository (AMMR) v.2.1.1 were adapted separately to calculate the respective kinematic variables (i.e., joint angles) and kinetic variables (i.e., joint reaction forces, joint moments, and muscle forces) of interest.

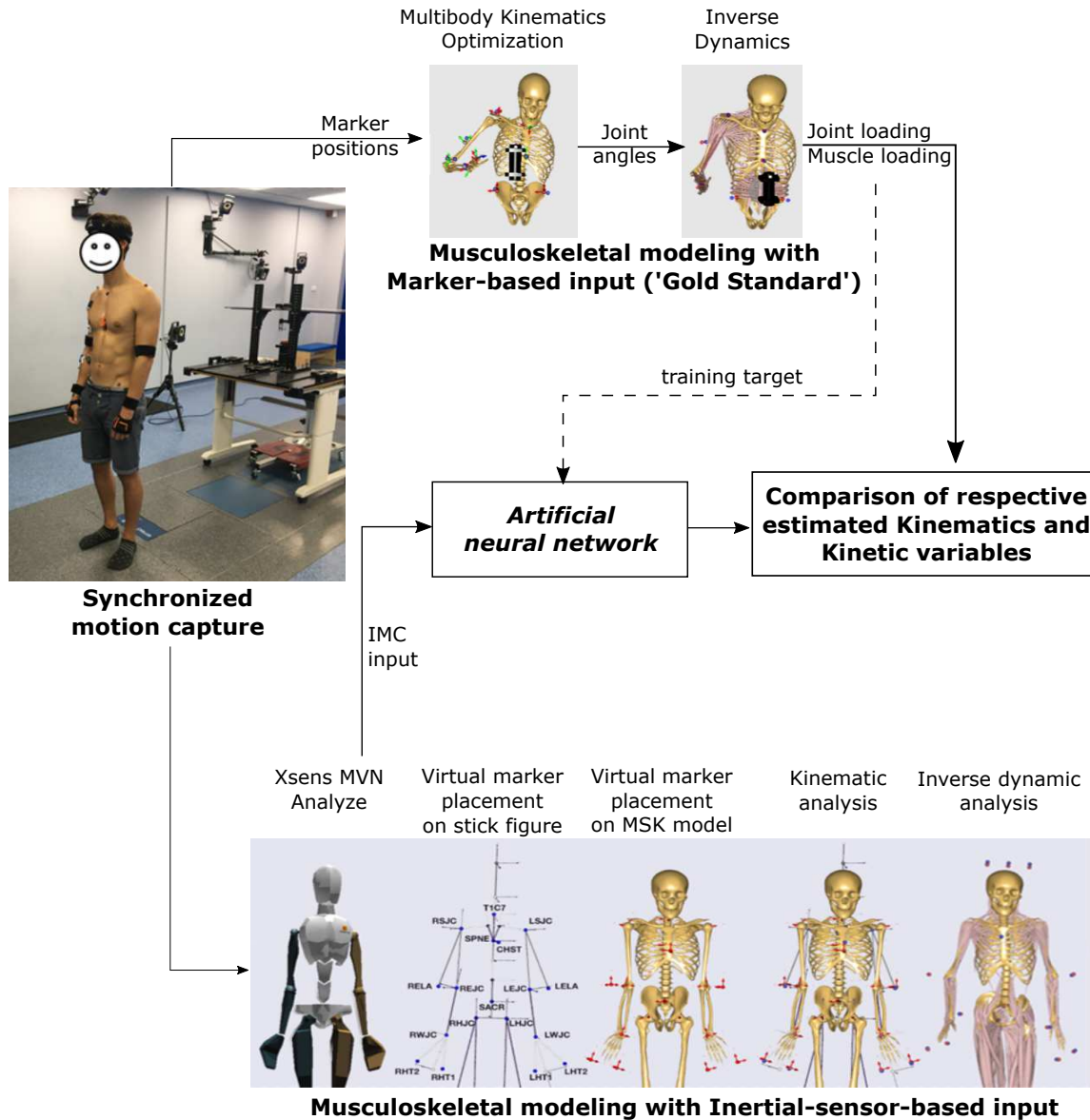


Figure 1: Pipeline for machine learning for musculoskeletal modeling of the upper extremity combining the marker-based and inertial-sensor-based motion capture inputs; Image adapted from [56, 17, 20, 36]

Demographic and anthropometric characteristics (e.g., age, height, body weight, gender) were found to influence the amplitude of kinematic and kinetic variables in clinical movement analysis, and if not corrected, individual differences may act as confounding factors [57, 58]. Therefore, the kinetic outcome variables were reported per the recommendations by the *International Society of Biomechanics* on reporting intersegmental forces and moments during human motion analysis [58]. In this study, the joint reaction force and muscle force values were normalized to the corresponding subject's body weight and were expressed as a percentage of body weight (%Body Weight [%BW]) to facilitate inter-individual comparison [59]. The joint moment values were normalized to the corresponding subject's body weight times height and were expressed as a percentage of body weight times body height (%Body Weight  $\times$  Body Height [%BW $\times$ BH]), since the 'body weight times height' normalization method was found to be more effective in reducing differences primarily due to gender than the 'body weight' normalization method [57]. The sign convention adopted for the joint angles was – Flexion (Fl), Forward bending (Fb), Abduction (Ab), Right bending (Rb), Radial deviation (Rd), and Internal rotation (Int) are positive (+ve); Extension (Ex), Backward bending (Bb), Adduction (Ad), Left bending (Lb), Ulnar deviation (Ud), and External rotation (Ext) are negative (-ve) [48].

Detailed instructions and a couple of practice sessions were provided for each subject prior to data collection. First, a calibration sequence was performed for the IMC mocap system, which involved the participants standing in a neutral posture ('N-pose') and walking a few steps forward and back to the starting position. Next, participants performed a 'static' trial by standing in a stationary neutral or anatomical position in the center of the capture volume for the OMC system. This was followed by three trials of the Reach-to-Grasp task with the subject's dominant hand at a self-selected pace. Execution of the task involved moving the hand from the 'Start/End' position to grasp the 'dumbbell'-shaped object from the 'Middle' block and placing it on the 'Front' block, then without letting go of the object, the hand would follow the same instructions/path in the return phase, and then the hand would return to the 'Start/End' location. In contrast with an earlier similar study solely involving MSK modeling with OMC input [56], the weight of the grasp object ('dumbbell') was considered to be a point object with negligible mass in the current MSK output involving the IMC or OMC data [20]. Notably, this assumption does not affect the objectives of the current study. The experimental data captured from the IMC system and the OMC-data driven MSK model estimations (i.e., kinematic and kinetic parameters) were used as training data for our ML endeavors.

## 2.2 Supervised learning

Recent studies concerning MSK modeling [60, 34, 44, 36] have shown the utility of NN architectures in bypassing MSK models driven individually by OMC or IMC inputs. In contrast to previous research that mapped IMC inputs to IMC-driven MSK outputs or OMC inputs to OMC-driven MSK outputs, we developed a novel ML model to obtain OMC-driven MSK outputs from IMC inputs for the human upper extremity (Figure 1).

As detailed in Section 2.1, the OMC data and IMC data are sampled at different frequencies; we down-sampled the OMC-driven MSK output using linear interpolation to match IMC data's sampling frequency (60 Hz). The IMC experimental data comprise 15 trials (i.e., three trials of Reach-to-Grasp task each obtained from the five subjects) with 483 input features [51] while the five OMC-driven MSK output feature categories comprise time-series of ten joint angles, twelve joint reaction forces, ten joint moments, four muscle forces, and four muscle activations. We train different ML models for each of the OMC-driven MSK model kinematic and kinetic output categories while using IMC experimental data as input.

We apply the following feature transformations, similar to those in our previous article [36] before training the model:

1. The time column, normalized between zero and one, represents the fraction of the total time elapsed for completing the task at a self-selected pace. This helps capture the temporal aspect of MSK analyses.
2. Muscles are typically discretized into numerous muscle bundles in MSK models. MSK model outputs for muscle forces and muscle activations comprise features for the four considered superficial muscle groups, i.e., (a) Pectoralis major (Clavicle part); (b) Biceps Brachii; (c) Deltoid (Medial); and (d) Brachioradialis [56]. The 'maximum envelope' of the tendon forces of selected bundles constituting a particular muscle was calculated for further analysis. The muscle activation is a measure of the force in a selected muscle relative to its strength.

To show the added utility of applying complex NNs, we first attempt a linear model to see if it provides satisfactory metrics. For both the linear and NN models, a thorough hyperparameter search is performed, across initialization, optimizer, batch-size, learning rate, and epochs.

We use Pearson's correlation coefficient ( $r$ ) and Normalized root-mean-squared error (NRMSE) metrics to compare the effectiveness of our models. For *subject-exposed* (SE) models, linear models perform 'moderately' to 'strongly' in terms of  $r$  (see Subsection 2.4). For *subject-naive* (SN) models, linear models perform moderately in terms of  $r$ , however, the NRMSE is large for SN models (as shown and discussed in Table 2 as well as Sections 3 and 4).

Therefore, it was concluded that complex ML models are necessary. A feed-forward backpropagation NN architecture was chosen with NRMSE as the cost function. Figure 2 shows a typical schematic diagram of NN used, with  $I$  input units,  $O$  output units, and  $N$  hidden layers with  $k$  neurons each. It should be noted that no activation was used in the final layer of the NN architecture. Moreover, validation accuracy was used to tune NN hyperparameters and perform an exhaustive search in the space with  $n = 43,740$  points. For the grid parameters in the hyperparameter search, we chose weight initialization, optimizer, batch-size, epoch, activation function, number of nodes, hidden layers, learning rate, and dropout probability as listed in Table 1. The current hyperparameter exploration is informed by our previous related work [36].

## 2.3 Validation and train-test split

Two approaches are commonly used to benchmark MSK ML models: *subject-exposed* (SE) and *subject-naive* (SN) [60]. The trials of all subjects are pooled together in the SE setting, and a train-test split is performed on the trials,

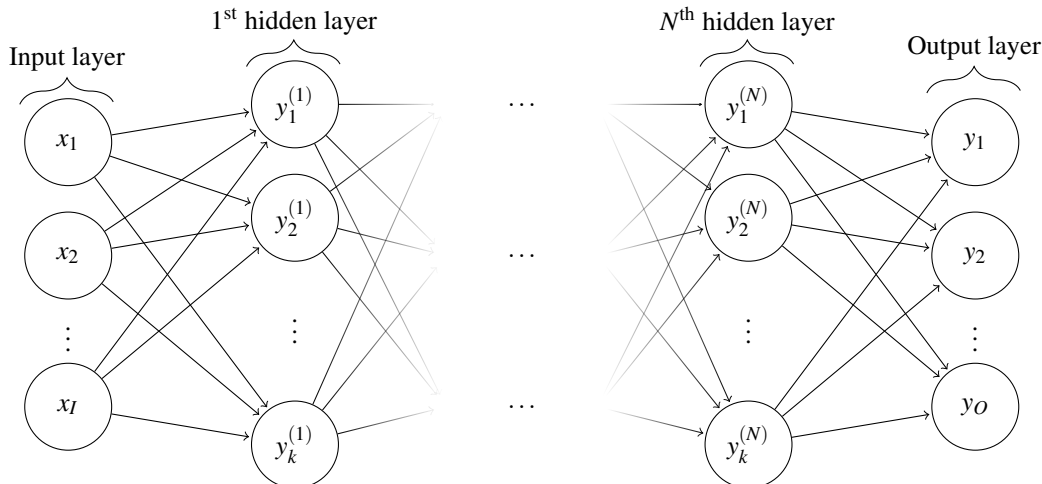


Figure 2: Typical schematic diagram for a feed-forward backpropagation Neural Network with  $I$  input units,  $O$  output units, and  $N$  hidden layers each containing contains  $k$  neurons. The input and output layers are considered as  $0^{\text{th}}$  and  $(N + 1)^{\text{th}}$  layers.

Output	Weight initialization	Optimizer	Batch size	Epoch	Activation function	Number of nodes	Hidden layers	Learning rate	Dropout probability
<b>Hyperparameters space explored</b>									
	Xavier normal	Adam	64	50	ReLU	200 to 1800	2, 4,	0.001	0
	Random normal	SGD	256	100	tanh	in steps of 200	6, 8, 10	0.005	0.2
	He normal	RMSProp	1028	200	sigmoid				
<b>Optimal hyperparameters in Subject-exposed settings</b>									
Joint angles	Random normal	Adam	256	200	ReLU	200	2	0.001	0.0
Joint reaction forces	Xavier normal	Adam	256	100	ReLU	200	8	0.005	0.0
Joint moments	Xavier normal	Adam	64	50	sigmoid	1400	2	0.001	0.2
Muscle forces	Random normal	SGD	64	50	ReLU	400	8	0.005	0.0
Muscle activations	Xavier normal	Adam	256	100	ReLU	1000	6	0.005	0.0
<b>Optimal hyperparameters in Subject-naive settings</b>									
Joint angles	Random normal	Adam	256	100	ReLU	800	4	0.005	0.0
Joint reaction forces	Random normal	Adam	256	50	ReLU	800	8	0.001	0.0
Joint moments	Xavier normal	Adam	64	50	sigmoid	1800	2	0.001	0.2
Muscle forces	Xavier normal	SGD	64	200	ReLU	1200	8	0.005	0.2
Muscle activations	Random normal	Adam	256	200	ReLU	1200	6	0.001	0.2

Table 1: Hyperparameters choices explored (43,740) for the neural networks along with optimal hyperparameters for each output categories in subject-exposed and subject-naive settings.

ensuring that each subject in the test set has at least one trial in the training set. This approach usually performs better than the SN setting, where a subject is strictly either in training or test data. While the performance is better, the SE model has the disadvantage of being a subject-specific model and does not generalize well [34].

In train-test split for the SE case, two trials were randomly selected as the test set and the remaining trials as the training set. For hyperparameter tuning, we performed cross-validation by randomly splitting the remaining 13 trials into validation (two trials) and training set (11 trials). While in the SN case, one of the subjects was randomly selected as the test subject and the remaining subjects as the training data. Subsequently, cross-validation was performed by randomly selecting one subject as the validation data and the remainder as the training data.

Output	Linear Model		Neural Network	
	$r_{\text{avg}}$ Mean (SD)	NRMSE <sub>avg</sub> Mean (SD)	$r_{\text{avg}}$ Mean (SD)	NRMSE <sub>avg</sub> Mean (SD)
<b>Subject-exposed</b>				
Joint angles	0.85 (0.15)	0.64 (0.62)	0.92 (0.23)	0.25 (0.20)
Joint reaction forces	0.77 (0.21)	0.70 (0.31)	0.91 (0.12)	0.34 (0.11)
Joint moments	0.83 (0.11)	0.58 (0.22)	0.88 (0.08)	0.41 (0.20)
Muscle forces	0.69 (0.28)	1.08 (0.30)	0.84 (0.30)	0.37 (0.17)
Muscle activations	0.75 (0.28)	0.74 (0.28)	0.88 (0.25)	0.29 (0.15)
<b>Subject-naive</b>				
Joint angles	0.89 (0.10)	2.07 (2.45)	0.86 (0.17)	0.83 (0.64)
Joint reaction forces	0.57 (0.47)	1.32 (1.30)	0.77 (0.31)	0.87 (0.79)
Joint moments	0.86 (0.10)	1.82 (1.37)	0.87 (0.09)	0.84 (0.57)
Muscle forces	0.76 (0.14)	1.72 (1.36)	0.94 (0.04)	0.49 (0.53)
Muscle activations	0.73 (0.10)	1.84 (0.87)	0.93 (0.04)	0.36 (0.24)

Table 2: Average Pearson’s correlation coefficient and average NRMSE values for Linear Model prediction and Neural Network prediction compared with Musculoskeletal model outputs. The NN model consistently outperforms the linear model. For a given output category, averaging is done over all output features and test trials. See Supplementary Table 1 for details.

## 2.4 Error metrics

NRMSE (i.e., RMSE scaled by the standard deviation of the variable in the dataset) was used as our primary error metric as in [36, 34], where the ground truth is the corresponding OMC-driven MSK output. Since RMSE (and thus NRMSE) is sensitive to outliers, we also used Pearson’s correlation coefficients ( $r$ ) between the MSK model outputs and the ML model-predicted outputs as a secondary measure. Here, we used the standard interpretation [61] for  $r$ : “weak” ( $r \leq 0.35$ ), “moderate” ( $0.35 < r \leq 0.67$ ), “strong” ( $0.67 < r \leq 0.90$ ), and “excellent” ( $r > 0.90$ ).

## 3 Results

Table 2 reports the mean  $r$  and NRMSE values for each kinematic and kinetic output category (where the mean is over all output features in a particular category) for feed-forward neural networks (NN) and linear models. The NN model consistently outperformed the linear model, and the SE models performed better than the SN models as expected. In particular, linear model performed reasonably well for SE settings, however, in comparison to our previous work [36] mapping IMC inputs to IMC-driven MSK outputs, the performance of linear model has considerably reduced.

Performing a rigorous hyperparameter search is essential to achieving good model fit and generalizability. We searched 43,740 combinations of hyperparameters in hyperparameter space as listed in Table 1. Cross-validation was performed for each hyperparameter choice, and the model with the best validation accuracy was selected. The best-performing model was then re-trained with the training and validation data, with the final metrics reported on a held-out test dataset. We obtained the best performance for the NNs with multiple hidden layers (greater than four in most cases) and wide layers containing up to 1800 nodes with the network initialized using either Xavier or Random normal initialization and parameters trained using ReLU activation function (on hidden layers), Adam optimizer, dropout regularization and a learning rate of 0.001/0.005.

For the NN models with the best fit, we obtained high correspondence, particularly for SE ( $r_{\text{avg}} = 0.89$  and  $\text{NRMSE}_{\text{avg}} = 0.33$ ), as compared to the best performance for SN setting ( $r_{\text{avg}} = 0.87$  and  $\text{NRMSE}_{\text{avg}} = 0.68$ ). In general, we expect SN performance to be worse than that for the SE case [36, 34].

To aid interpreting the results, Figures 3–7 show the correspondence between the NN-predicted outputs and the actual MSK outputs for the test set. Most plots show excellent  $r$  ( $> 0.85$ ) with notable exceptions, particularly for SN settings, in case of Elbow Mediolateral, Elbow Anteroposterior, and Trunk Mediolateral (joint reaction forces) and Trunk Flexion/Extension and Trunk Internal/External rotation (joint moments). For further information, we have tabulated with maximum, minimum, and inter-quartile ranges for  $r_{\text{avg}}$  and  $\text{NRMSE}_{\text{avg}}$  for all output features in Supplementary Table 1. Moreover, in Supplementary Table 2, we have provided  $\text{RMSE}_{\text{avg}}$  (with units) that given an absolute error in the prediction of a given MSK output. Note that the interpretation of RMSE values comes with the caveat that different features cannot be compared directly due to their different scales.

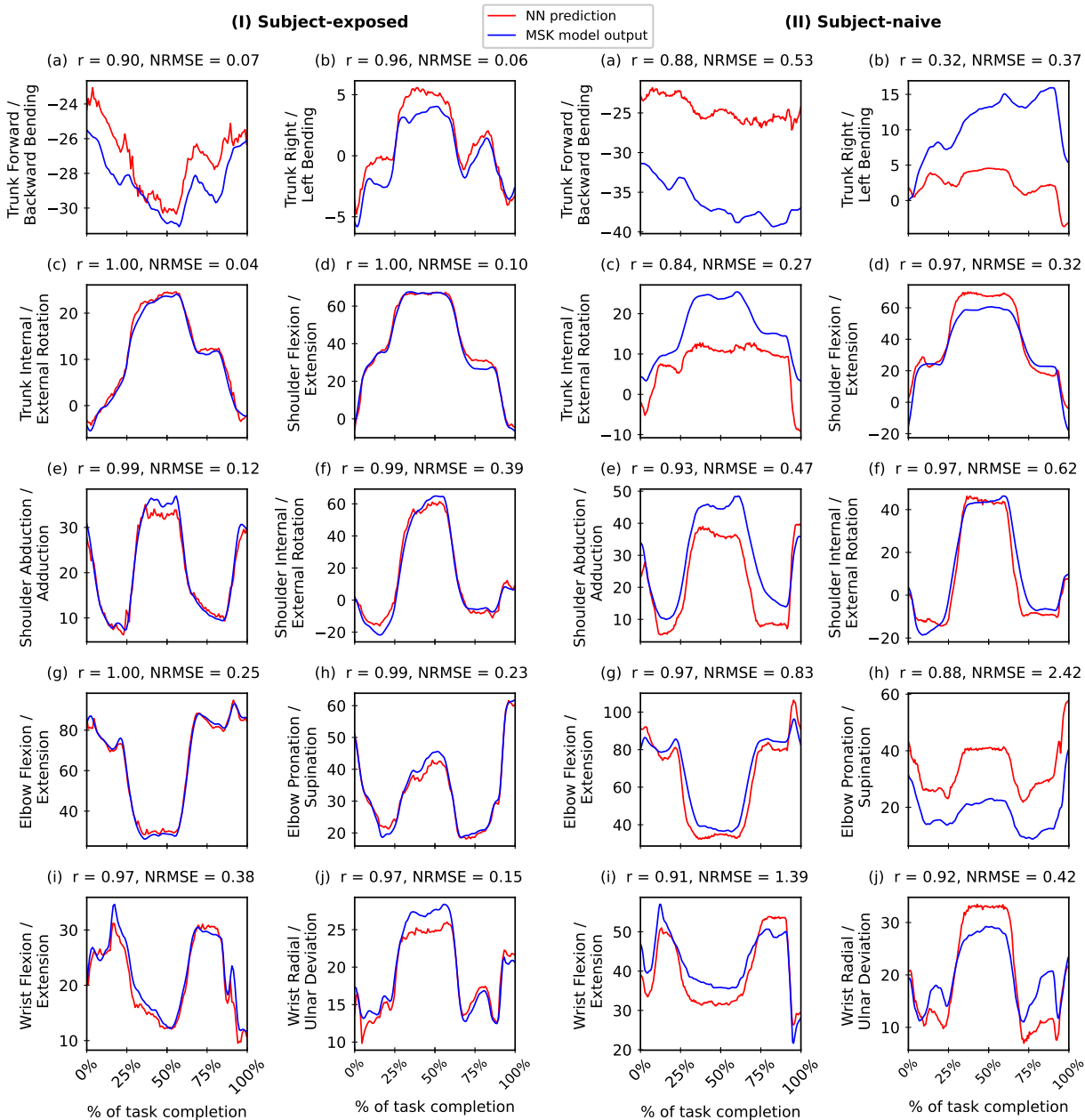


Figure 3: Comparing neural network (NN) predictions for joint angles (in degrees) with the corresponding musculoskeletal (MSK) model outputs on a test trial in *Subject-exposed* (left) and *Subject-naive* (right) settings.

## 4 Discussion

Here, an ML method is introduced to estimate OMC-driven MSK model outputs from experimental data synchronously captured from an IMC system. This has the dual advantage of bypassing the computationally expensive MSK model and obtaining the corresponding OMC-driven MSK output while not needing the laborious and laboratory-bound (non-invasive ‘gold standard’) OMC setup. The full-body IMC system provides unprecedented ease of use, high-quality data (in near-real time), and a relatively short setup time. The same ease of use translates to setting up the MSK modeling pipeline driven by the IMC data. Compared to OMC data capture, this approach saves time to skillfully palpate bony landmarks for marker placement and cumbersome post-processing of markers or missing data.

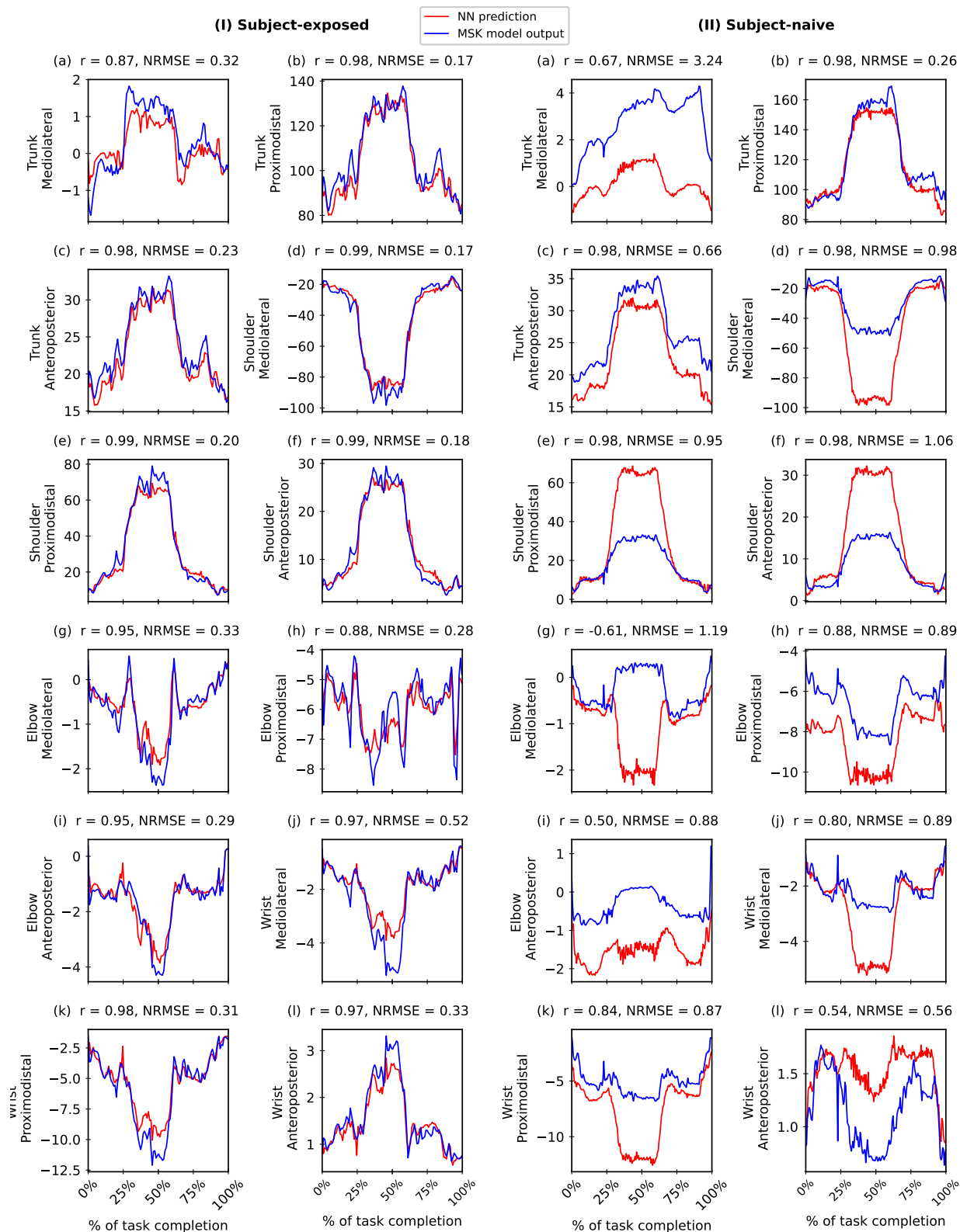


Figure 4: Comparing neural network (NN) predictions for joint reaction forces (% Body Weight) with corresponding musculoskeletal (MSK) model outputs on a test trial in *Subject-exposed* (left) and *Subject-naive* (right) settings.

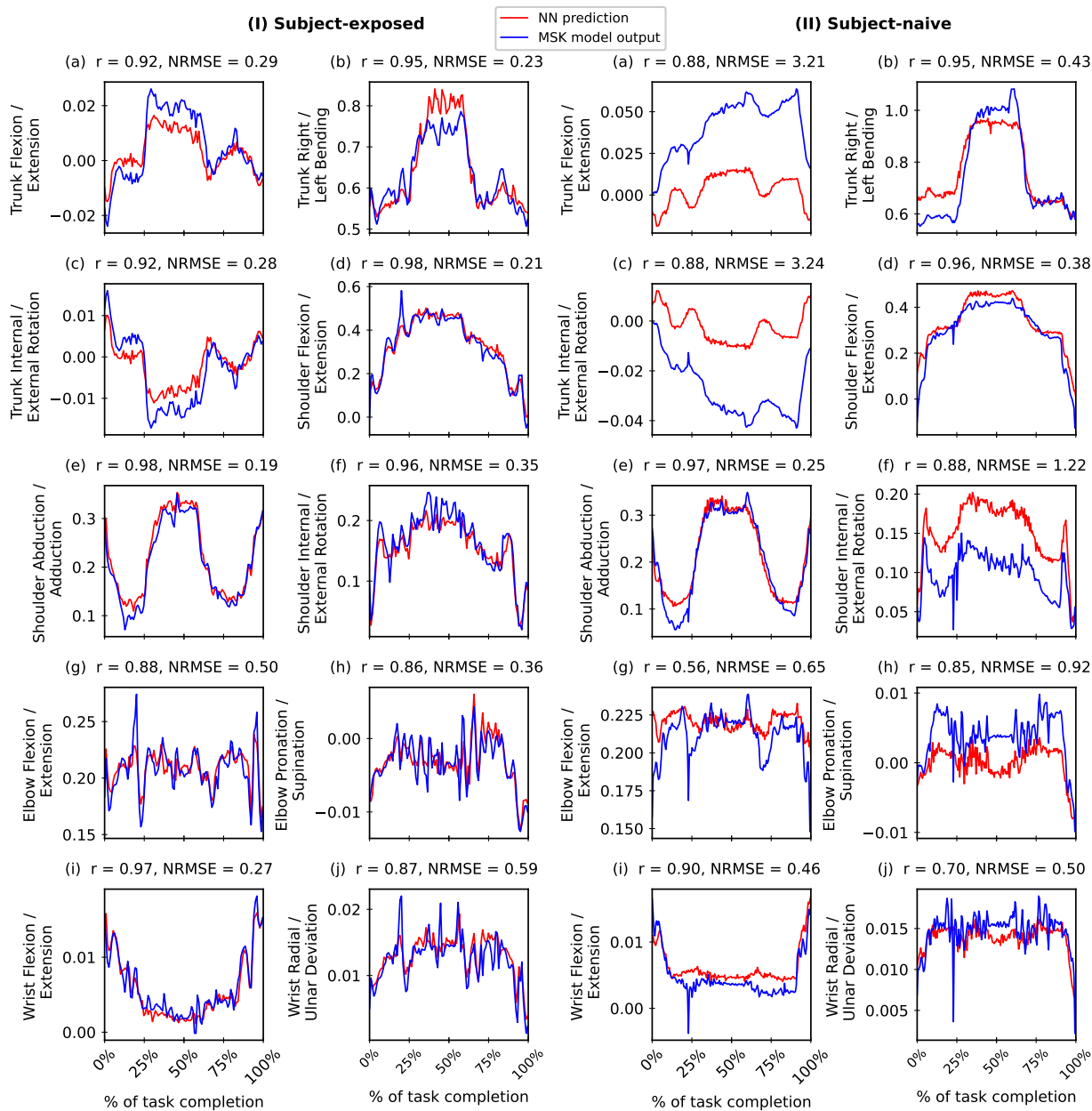


Figure 5: Comparing neural network (NN) prediction for joint moments (% Body Weight  $\times$  Body Height) with the corresponding musculoskeletal (MSK) model outputs on a test trial in *Subject-exposed* (left) and *Subject-naive* (right) settings.

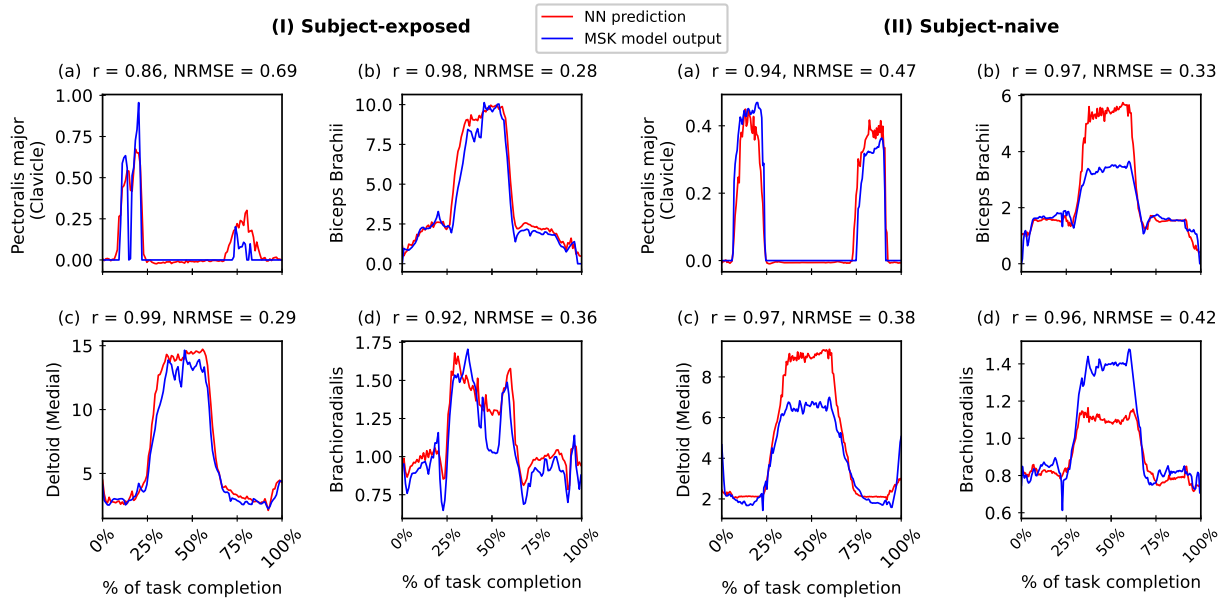


Figure 6: Comparing neural network (NN) predictions for muscle forces (% Body Weight) with the corresponding musculoskeletal (MSK) model outputs for a test trial in *Subject-exposed* (left) and *Subject-naive* (right) settings.

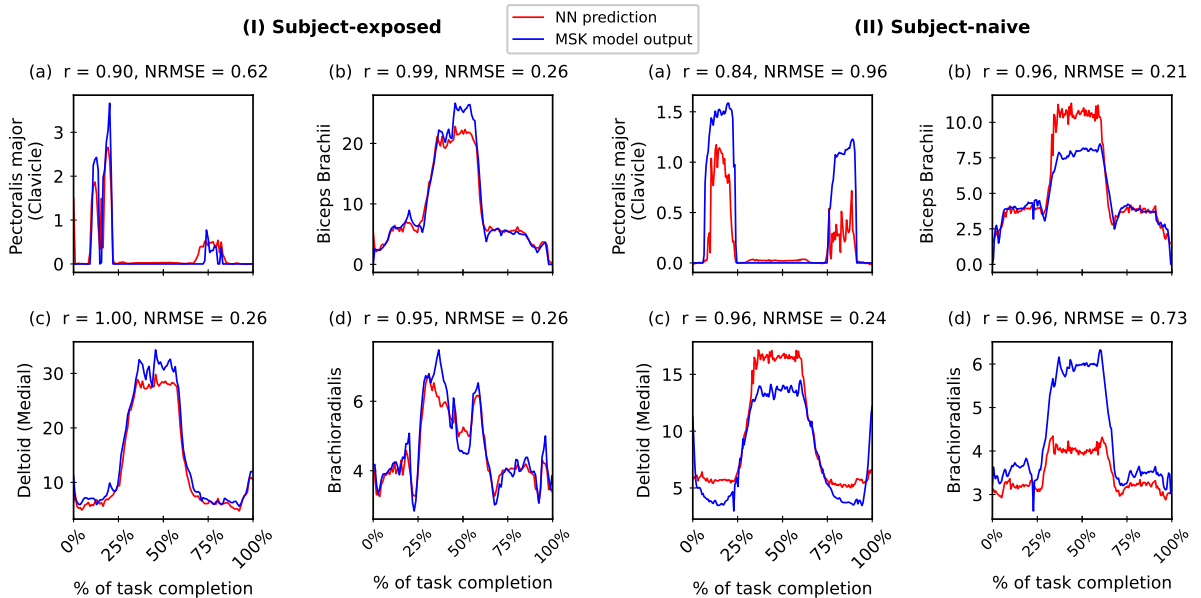


Figure 7: Comparing neural network (NN) predictions for muscle activations (%) with the corresponding musculoskeletal (MSK) model outputs for a test trial in *Subject-exposed* (left) and *Subject-naive* (right) settings.

We considered both SN and SE scenarios – considering both are important [27], as the choice affects generalizability, and thus, model accuracy [34, 60, 62]. While SE models tend to perform better, they are not as generalizable to unseen subjects as SN models. SE models can incorporate subject-specific tendencies to better predict kinematic and kinetic variables corresponding to them. Various architectures were used, ranging from a simple linear model to NNs. While the linear model was adequate for SE, as expected, it could not reproduce results well in the SN case. As opposed to our previous work [36], the discrepancy in metrics between linear models and NN in this study is substantial, even for SE setting, which might be attributed to the greater complexity of the mapping OMC-based MSK model output to IMC input. Subsequently, we considered more complex architectures such as the feed-forward NN, similar to Sharma et al. [36]. In contrast to previous works [60, 34], we conducted a thorough hyperparameter search which improves model fit and generalizability as found in [36]. We obtained good model performance in both scenarios (Table 2).

In general, we obtained an excellent correspondence in the NN prediction and the ground truth i.e., OMC-driven MSK output with some notable exceptions, in particular, for SN settings. Some of these issues could be attributed to the lack of adequate training data (we have  $N = 5$ ), which we hope to address in future work by adding subjects and considering synthetic data augmentation using biomechanical models [63, 45, 64].

As a result of the experiment being conducted in a laboratory setting, good model performance does not necessarily imply ecological validity in terms of replication in a real-world setting. Though the experiment task is a constrained, cyclical, goal-oriented Reach-to-Grasp task that is ubiquitous in everyday life [56], it may not necessarily generalize to other settings. While a study [60] involving ML models on the lower extremity has shown generalizability across age and body morphologies (and thus gait), this may not be the case for the upper extremity because of a larger range of motions, higher degrees of freedom, and three-dimensional nature of tasks [1, 2]. The applicability of our model for *what-if* analyses involving the task with different object weights or differently-shaped objects and other upper-extremity motions are yet to be explored.

Previously, ML was shown to predict IMC-driven MSK model outputs with high accuracies using IMC data [36]. However, the performance of linear models and NNs is relatively lower in the present study. Notably, both OMC and IMC mocap systems are prone to soft tissue artifacts [65, 9] and instrumental errors [66] differently, which often leads to differences in pose estimation accuracy between the measurement systems (e.g., tracking long-axis rotations like shoulder internal/external rotation or elbow pronation/supination). In particular, IMC systems are more susceptible to soft tissue artifacts (i.e., at least three passive markers placed on bony landmarks of a segment [in an OMC system] versus one IMU placed in the middle of the body segment [in an IMC system]). Hence, the ML model performance (in this study versus our prior study [36]) needs to be interpreted within this context. In this study, the map from IMC input (inherently lower-quality inputs) to OMC-derived MSK outputs (corresponding to higher-quality OMC inputs) is more complex. Our observations also corroborate that the NN models implemented in this study are more complicated (Table 1), generally requiring more hidden layers and neurons than a similar previous study [36]. Further, in the current study, the NN models considerably outperform the linear models in contrast to Sharma et al. [36].

So far, we have focused on this study’s utility in (i) bypassing the computationally expensive MSK model and (ii) obtaining gold-standard OMC-driven MSK outputs from IMC inputs. However, more recent alternative methods such as inverse kinematics, inverse dynamics, and static optimization can do real-time data processing, thus alleviating one of the main issues with using MSK models, especially in field situations. While these are valuable alternatives to the MSK model or even an ML model that emulates MSK modeling like this study, these approaches can only obtain efficiency by sacrificing accuracy and simplifying the model. For example, taking tendon compliance into account is essential in research that relies on the muscle-tendon interaction or stored elastic energy in tendons (e.g., in running) [67], and helps achieve human-like motion [68, 69]. Such aspects are ignored in ‘real-time’ inverse dynamics. To achieve real-time performance, simplified models are numerically solved up to a small number of iterations, which decreases accuracy. Predictions improve if the models are allowed to run longer, such as in offline scenarios [70, 71, 72]. Thus these alternative methods cannot be generalized easily and encode assumptions about certain movements that make them limited. In contrast, NN models are flexible while offering accuracy and speed. The trade-off between speed and accuracy in modern non-ML-based alternatives to MSK models is an interesting question that we hope to return to in future work.

Our work relies on MSK models, and thus, it inherits some of the underlying limitations, such as not considering soft-tissue artifacts [73, 74, 75]. While MSK models are a standard method to obtain kinematics and kinetics from motion capture, work is ongoing [3, 76, 67, 77] in MSK model verification & validation (V&V). V&V aims to address the limitations of the MSK model in terms of accuracy concerning higher fidelity sources such as bone-pin marker measurements [78], which minimize the impact of soft-tissue artifacts. Direct measurements in general [79, 80] and *in vivo* joint reaction forces [59, 81, 82] using endoprosthesis have been used to validate the MSK model. Any future improvements in the MSK model from such V&V efforts will improve ML predictions based on MSK models, like in this work.

This work can be used as a starting point toward implementing ‘lab-to-field’ approach by using ML modeling on easily obtained IMC data. This can be used for translational research that uses MSK model outputs on IMC data obtained in real-world settings such as supermarkets and manual material handling [83, 22, 84, 21, 85] as a training corpus for an ensemble of ML models which can be used to facilitate clinical diagnosis rapidly. In addition to IMC data, recent work on markerless systems [86], such as two-dimensional recordings [44], to obtain mocap quality data provides another source of training data while being used without specialized equipment.

## 5 Study limitations

Our study’s key limitation is the small sample size of  $N = 5$ ; nevertheless, the methodological framework introduced in this proof-of-concept study shows that it is possible to get ‘OMC-quality’ MSK model estimations reasonably from comparatively lower-quality IMC measurements and paves the way for more elaborate studies going forward. Many studies in this field have considered up to  $N = 10$  subjects [27]. Future studies should involve a larger sample size and training dataset to help with improved predictions and a more generalizable model. V&V of MSK models is a non-trivial endeavor and has remained a crucial topic of ongoing research [3, 76, 67, 77]. Consequently, further improvements of MSK model V&V could result in more accurate kinematic and kinetic estimates and thereby help perform better ML-based predictions. Even though our approach to mapping highly portable IMC inputs to (non-invasive gold standard) OMC input-driven MSK outputs is unique, the training of such ML models is limited to synchronized IMC and OMC data capture to create the train and test datasets. One workaround is to perhaps use synthetic IMU data in training the ML models, as demonstrated earlier [46].

## 6 Recommended future work

We see relevant future work proceeding broadly along three lines of inquiry. Firstly, we can incorporate our ML pipelines (presented here and earlier [36]) in relevant open-source tools [87, 88] with a graphical user interface. These interfaces can assist users in estimating kinematic and kinetic variables of interest from mocap data without needing an MSK modeling framework. Secondly, utilizing the ML model on larger datasets and potentially working with open-access mocap data. An example of such data validated with *in vivo* instrumented devices is from the Grand Knee Challenge [79, 80]. Another prominent repository is the CMU Motion Capture Dataset [89] – one of the largest publicly available mocap datasets. Thirdly, we are planning to expand the study to consider other ML architectures for upper-extremity biomechanical modeling, e.g., Gaussian Processes, which have been found in areas such as robotics [90, 91] and ergonomics [92]. This would be particularly beneficial in *subject-naive* settings where there is room for improvement. The benefit of Gaussian Processes compared to NNs is one obtains information about uncertainty in predictions automatically. Performance comparison with different ML techniques, e.g., Support Vector Regression, should also be considered. (e.g., methods listed by [27, 35, 41]). Undertaking methodological variations on the NN approach, such as comparing various NN frameworks and assessing their suitability for different tasks [93], can be considered. Future studies could also explore an ML model’s robustness in the presence of artificial noise or contamination.

## 7 Conclusion

To the authors’ knowledge, this is the first-ever study (across lower and upper-extremity) that uses experimental data captured from an IMC system to directly estimate OMC-driven MSK model outputs (kinematic and kinetic) using an ML approach to bypass the need for (lab-based) OMC system *and* computationally expensive MSK model. This was achieved by following ML best practices, such as an extensive hyperparameter search and utilizing dropout for regularization. Such models can act as viable alternatives to the MSK modeling process requiring OMC input data, which are superior to predictive models that use only IMUs. The efficiency and accuracy of the ML models make it viable as an accessible and affordable solution, especially in resource-austere settings, for taking motion analysis and MSK modeling *beyond the lab* to the real world.

## Data availability

The datasets presented here are not readily available due to ethical and privacy reasons. The Python codes used for NN implementation and data analysis here as well as the test data are available on [https://github.com/rahu12512/MSK\\_ML\\_beta](https://github.com/rahu12512/MSK_ML_beta).

## Author Contributions

VHN and CM conceived the project. VHN conceptualized the biomechanical methodology, and developed the anonymized dataset. CM conceptualized the ML methodology. RS, AD, CM, and VHN contributed to data processing and development of the ML models. RS developed the ML methodology and implemented the codes for ML and analysis with contributions from CM and AD. RS, AD, CM, and VHN contributed in the analysis and writing of final results. All authors contributed to drafting, review, and editing. All authors have read and agreed to the final version of the manuscript.

## Acknowledgment

This project has benefited from the dataset acquired for a previous project that was funded through the *Research Councils UK (RCUK) Digital Economy Programme grant number EP/G036861/1* (Oxford Centre for Doctoral Training in Healthcare Innovation) and the *Wellcome Trust Affordable Healthcare in India Award (Grant number 103383/B/13/Z)*. CM is supported by a Fellowship with the Accelerate Program for Scientific Discovery at the Computer Laboratory, University of Cambridge. We are grateful to the *Swiss National Science Foundation 200020 182184* (RS) and *SCITAS, EPFL* for computational resources.

## References

- [1] G Rau, C Disselhorst-Klug, and R Schmidt. Movement biomechanics goes upwards: From the leg to the arm. *Journal of Biomechanics*, 33(10):1207–1216, 2000.
- [2] Carolyn Anglin and UP Wyss. Review of arm motion analyses. *Proceedings of the Institution of Mechanical Engineers, Part H: Journal of Engineering in Medicine*, 214(5):541–555, 2000.
- [3] Ahmet Erdemir, Scott McLean, Walter Herzog, and Antonie J van den Bogert. Model-based estimation of muscle forces exerted during movements. *Clinical Biomechanics*, 22(2):131–154, 2007.
- [4] Adam D Sylvester, Steven G Lautzenheiser, and Patricia Ann Kramer. A review of musculoskeletal modelling of human locomotion. *Interface Focus*, 11(5):20200060, 2021.
- [5] Bryce A Killen, Antoine Falisse, Friedl De Groote, and Ilse Jonkers. In silico-enhanced treatment and rehabilitation planning for patients with musculoskeletal disorders: Can musculoskeletal modelling and dynamic simulations really impact current clinical practice? *Applied Sciences*, 10(20):7255, 2020.
- [6] Ivo Roupá, Mariana Rodrigues da Silva, Filipe Marques, Sérgio B Gonçalves, Paulo Flores, and Miguel Tavares da Silva. On the modeling of biomechanical systems for human movement analysis: A narrative review. *Archives of Computational Methods in Engineering*, pages 1–44, 2022.
- [7] Samuel HL Smith, Russell J Coppack, Antonie J van den Bogert, Alexander N Bennett, and Anthony MJ Bull. Review of musculoskeletal modelling in a clinical setting: Current use in rehabilitation design, surgical decision making and healthcare interventions. *Clinical Biomechanics*, page 105292, 2021.
- [8] Benjamin J Fregly. A conceptual blueprint for making neuromusculoskeletal models clinically useful. *Applied Sciences*, 11(5):2037, 2021.
- [9] Huiyu Zhou and Huosheng Hu. Human motion tracking for rehabilitation—A survey. *Biomedical Signal Processing and Control*, 3(1):1–18, 2008.
- [10] Muhammad Yahya, Jawad Ali Shah, Kushsairy Abdul Kadir, Zulkhairi M Yusof, Sheroz Khan, and Arif Warsi. Motion capture sensing techniques used in human upper limb motion: A review. *Sensor Review*, 2019.
- [11] Aurelio Cappozzo, Ugo Della Croce, Alberto Leardini, and Lorenzo Chiari. Human movement analysis using stereophotogrammetry: Part 1: Theoretical background. *Gait & Posture*, 21(2):186–196, 2005.
- [12] Erik Jung, Cheryl Lin, Martin Contreras, and Mircea Teodorescu. Applied machine learning on phase of gait classification and joint-moment regression. *Biomechanics*, 2(1):44–65, 2022.
- [13] Marco Iosa, Pietro Picerno, Stefano Paolucci, and Giovanni Morone. Wearable inertial sensors for human movement analysis. *Expert Review of Medical Devices*, 13(7):641–659, 2016.
- [14] Pietro Picerno, Marco Iosa, Clive D’Souza, Maria Grazia Benedetti, Stefano Paolucci, and Giovanni Morone. Wearable inertial sensors for human movement analysis: A five-year update. *Expert Review of Medical Devices*, pages 1–16, 2021.

- [15] Michael Damsgaard, John Rasmussen, Søren Tørholm Christensen, Egidijus Surma, and Mark De Zee. Analysis of musculoskeletal systems in the Anybody Modeling System. *Simulation Modelling Practice and Theory*, 14(8):1100–1111, 2006.
- [16] Scott L Delp, Frank C Anderson, Allison S Arnold, Peter Loan, Ayman Habib, Chand T John, Eran Guendelman, and Darryl G Thelen. OpenSim: Open-source software to create and analyze dynamic simulations of movement. *IEEE Transactions on Biomedical Engineering*, 54(11):1940–1950, 2007.
- [17] Angelos Karatsidis, Moonki Jung, H Martin Schepers, Giovanni Bellusci, Mark de Zee, Peter H Veltink, and Michael Skipper Andersen. Musculoskeletal model-based inverse dynamic analysis under ambulatory conditions using inertial motion capture. *Medical Engineering & Physics*, 65:68–77, 2019.
- [18] Angelos Karatsidis, Giovanni Bellusci, H Martin Schepers, Mark De Zee, Michael S Andersen, and Peter H Veltink. Estimation of ground reaction forces and moments during gait using only inertial motion capture. *Sensors*, 17(1):75, 2017.
- [19] Jason M Konrath, Angelos Karatsidis, H Martin Schepers, Giovanni Bellusci, Mark de Zee, and Michael S Andersen. Estimation of the knee adduction moment and joint contact force during daily living activities using inertial motion capture. *Sensors*, 19(7):1681, 2019.
- [20] Vikranth H Nagaraja, Runbei Cheng, Emily (Man Ting) Kwong, Jeroen H. Bergmann, Michael S Andersen, and Mark S Thompson. Marker-based vs. inertial-based motion capture: Musculoskeletal modelling of upper extremity kinetics. In *ISPO Trent International Prosthetics Symposium (TIPS) 2019*, pages 37–38, Manchester, United Kingdom, 2019. ISPO.
- [21] Frederik Greve Larsen, Frederik Petri Svenningsen, Michael Skipper Andersen, Mark De Zee, and Sebastian Skals. Estimation of spinal loading during manual materials handling using inertial motion capture. *Annals of Biomedical Engineering*, 48(2):805–821, 2020.
- [22] Sebastian Skals, Rúni Bláfoss, Lars Louis Andersen, Michael Skipper Andersen, and Mark de Zee. Manual material handling in the supermarket sector. Part 2: Knee, spine and shoulder joint reaction forces. *Applied Ergonomics*, 92:103345, 2021.
- [23] Giacomo Di Raimondo, Benedicte Vanwanseele, Arthur Van der Have, Jill Emmerzaal, Miel Willems, Bryce Adrian Killen, and Ilse Jonkers. Inertial sensor-to-segment calibration for accurate 3d joint angle calculation for use in OpenSim. *Sensors*, 22(9):3259, 2022.
- [24] Jasper Verheul, Niels J Nedergaard, Jos Vanrenterghem, and Mark A Robinson. Measuring biomechanical loads in team sports—From lab to field. *Science and Medicine in Football*, 4(3):246–252, 2020.
- [25] David J Saxby, Bryce Adrian Killen, C Pizzolato, CP Carty, LE Diamond, L Modenese, J Fernandez, G Davico, M Barzan, G Lenton, et al. Machine learning methods to support personalized neuromusculoskeletal modelling. *Biomechanics and Modeling in Mechanobiology*, 19(4):1169–1185, 2020.
- [26] Fraser Philp, Robert Freeman, and Caroline Stewart. An international survey mapping practice and barriers for upper-limb assessments in movement analysis. *Gait & Posture*, 2022.
- [27] Eni Halilaj, Apoorva Rajagopal, Madalina Fiterau, Jennifer L Hicks, Trevor J Hastie, and Scott L Delp. Machine learning in human movement biomechanics: Best practices, common pitfalls, and new opportunities. *Journal of Biomechanics*, 81:1–11, 2018.
- [28] Liangliang Xiang, Alan Wang, Yaodong Gu, Liang Zhao, Vickie Shim, and Justin Fernandez. Recent machine learning progress in lower limb running biomechanics with wearable technology: A systematic review. *Frontiers in Neurobotics*, 16, 2022.
- [29] Ilan Eskinazi and Benjamin J Fregly. Surrogate modeling of deformable joint contact using artificial neural networks. *Medical Engineering & Physics*, 37(9):885–891, 2015.
- [30] Marzieh M Ardestani, Mehran Moazen, Zhenxian Chen, Jing Zhang, and Zhongmin Jin. A real-time topography of maximum contact pressure distribution at medial tibiofemoral knee implant during gait: Application to knee rehabilitation. *Neurocomputing*, 154:174–188, 2015.
- [31] Frank J Wouda, Matteo Giuberti, Giovanni Bellusci, Erik Maartens, Jasper Reenalda, Bert-Jan F Van Beijnum, and Peter H Veltink. Estimation of vertical ground reaction forces and sagittal knee kinematics during running using three inertial sensors. *Frontiers in Physiology*, 9:218, 2018.
- [32] Marion Mundt, Arnd Koeppe, Sina David, Franz Bamer, Wolfgang Potthast, and Bernd Markert. Prediction of ground reaction force and joint moments based on optical motion capture data during gait. *Medical Engineering & Physics*, 86:29–34, 2020.

- [33] Bernard XW Liew, David Rügamer, Xiaojun Zhai, Yucheng Wang, Susan Morris, and Kevin Netto. Comparing shallow, deep, and transfer learning in predicting joint moments in running. *Journal of biomechanics*, 129:110820, 2021.
- [34] Georgios Giarmatzis, Evangelia I Zacharaki, and Konstantinos Moustakas. Real-time prediction of joint forces by motion capture and machine learning. *Sensors*, 20(23):6933, 2020.
- [35] Chang June Lee and Jung Keun Lee. Inertial motion capture-based wearable systems for estimation of joint kinetics: A systematic review. *Sensors*, 22(7):2507, 2022.
- [36] Rahul Sharma, Abhishek Dasgupta, Runbei Cheng, Challenger Mishra, and Vikranth H. Nagaraja. Machine learning for musculoskeletal modeling of upper extremity. *IEEE Sensors Journal*, 22(19), 2022.
- [37] Lisa Noteboom, Marco Hoozemans, Dirkjan Veeger, and Frans Van Der Helm. Feasibility and validity of a single camera CNN driven musculoskeletal model for muscle force estimation during upper extremity strength exercises: Proof-of-concept. *Frontiers in Sports and Active Living*, page 373, 2022.
- [38] Tian Tan, Dianxin Wang, Peter B Shull, and Eni Halilaj. Imu and smartphone camera fusion for knee adduction and knee flexion moment estimation during walking. *IEEE Transactions on Industrial Informatics*, 2022.
- [39] Megan V McCabe, Douglas W Van Citters, and Ryan M Chapman. Developing a method for quantifying hip joint angles and moments during walking using neural networks and wearables. *Computer Methods in Biomechanics and Biomedical Engineering*, pages 1–11, 2022.
- [40] Justin Fernandez, Alex Dickinson, and Peter Hunter. Population based approaches to computational musculoskeletal modelling, 2020.
- [41] Anurag Sohane and Ravinder Agarwal. Knee muscle force estimating model using machine learning approach. *The Computer Journal*, 2020.
- [42] S. T. Mubarrat and S. Chowdhury. Convolutional lstm: a deep learning approach to predict shoulder joint reaction forces. *Computer Methods in Biomechanics and Biomedical Engineering*, 0(0):1–13, 2022.
- [43] Wen Wu, Katherine R Saul, and He Helen Huang. Using reinforcement learning to estimate human joint moments from electromyography or joint kinematics: An alternative solution to musculoskeletal-based biomechanics. *Journal of Biomechanical Engineering*, 143(4), 2021.
- [44] Daniel J Cleather. Neural network based approximation of muscle and joint contact forces during jumping and landing. *Journal of Human Performance and Health*, 1:f1–f13, 2019.
- [45] Marion Mundt, Arnd Koeppe, Sina David, Tom Witter, Franz Bamer, Wolfgang Potthast, and Bernd Markert. Estimation of gait mechanics based on simulated and measured IMU data using an artificial neural network. *Frontiers in Bioengineering and Biotechnology*, 8, 2020.
- [46] Marion Mundt, Wolf Thomsen, Tom Witter, Arnd Koeppe, Sina David, Franz Bamer, Wolfgang Potthast, and Bernd Markert. Prediction of lower limb joint angles and moments during gait using artificial neural networks. *Medical & biological engineering & computing*, 58(1):211–225, 2020.
- [47] Vikranth Nagaraja, Jeroen Bergmann, Michael Skipper Andersen, and Mark Thompson. Compensatory movements involved during simulated upper limb prosthetic usage: Reach Task vs. Reach-to-Grasp Task. In *XV ISB International Symposium on 3-D Analysis of Human Movement*, Salford, United Kingdom, 2018. ISB.
- [48] Vikranth H. Nagaraja, Jeroen H.M. Bergmann, Michael S. Andersen, and Mark S. Thompson. Comparison of a scaled cadaver-based musculoskeletal model with a clinical upper extremity model. *Journal of Biomechanical Engineering*, 2022. Under review.
- [49] Vicon motion systems | Plug-in Gait Reference Guide – Vicon Documentation. <https://docs.vicon.com/display/Nexus212/Plug-in+Gait+Reference+Guide>. (Accessed on 12/04/2022).
- [50] Monique Paulich, Martin Schepers, Nina Rudigkeit, and Giovanni Bellusci. Xsens mtw awinda: Miniature wireless inertial-magnetic motion tracker for highly accurate 3D kinematic applications. *Xsens: Enschede, The Netherlands*, pages 1–9, 2018.
- [51] Xsens MVN User Manual. [https://www.xsens.com/hubfs/Downloads/usermanual/MVN\\_User\\_Manual.pdf](https://www.xsens.com/hubfs/Downloads/usermanual/MVN_User_Manual.pdf), 2021. (Accessed on 12/24/2021).
- [52] Xsens. Synchronising Xsens systems with Vicon Nexus, January 2020. (Accessed on 03/16/2021).
- [53] Vicon nexus™ 2.5 manual. 2016. what’s new in vicon nexus 2.5 – nexus 2.5 documentation. documentation docs.vicon.com. <https://docs.vicon.com/display/Nexus25/PDF+downloads+for+Vicon+Nexus?preview=/50888706/50889382/ViconNexusWhatsNew25.pdf>. (Accessed on 02/02/2022).

- [54] Motion Lab Systems. C3D.ORG - the biomechanics standard file format. <https://www.c3d.org/>. (Accessed on 08/16/2022).
- [55] MVN Analyze. <https://www.xsens.com/products/mvn-analyze>. (Accessed on 12/24/2021).
- [56] Vikranth Harthikote Nagaraja. *Motion capture and musculoskeletal simulation tools to measure prosthetic arm functionality*. PhD thesis, Department of Engineering Science, University of Oxford, Oxford, United Kingdom, 2019.
- [57] Kirsten C Moision, Dale R Sumner, Susan Shott, and Debra E Hurwitz. Normalization of joint moments during gait: A comparison of two techniques. *Journal of Biomechanics*, 36(4):599–603, 2003.
- [58] Timothy R Derrick, Antonie J van den Bogert, Andrea Cereatti, Raphaël Dumas, Silvia Fantozzi, and Alberto Leardini. ISB recommendations on the reporting of intersegmental forces and moments during human motion analysis. *Journal of Biomechanics*, 99:109533, 2020.
- [59] G Bergmann, F Graichen, A Bender, M Kääh, A Rohlmann, and P Westerhoff. In vivo glenohumeral contact forces—measurements in the first patient 7 months postoperatively. *Journal of Biomechanics*, 40(10):2139–2149, 2007.
- [60] Lance Rane, Ziyun Ding, Alison H McGregor, and Anthony MJ Bull. Deep learning for musculoskeletal force prediction. *Annals of Biomedical Engineering*, 47(3):778–789, 2019.
- [61] Richard Taylor. Interpretation of the correlation coefficient: A basic review. *Journal of Diagnostic Medical Sonography*, 6(1):35–39, 1990.
- [62] Marzieh M Ardestani, Zhenxian Chen, Ling Wang, Qin Lian, Yaxiong Liu, Jiankang He, Dichen Li, and Zhongmin Jin. Feed forward artificial neural network to predict contact force at medial knee joint: Application to gait modification. *Neurocomputing*, 139:114–129, 2014.
- [63] Eva Dorschky, Marlies Nitschke, Christine F Martindale, Antonie J van den Bogert, Anne D Koelewijn, and Bjoern M Eskofier. Cnn-based estimation of sagittal plane walking and running biomechanics from measured and simulated inertial sensor data. *Frontiers in Bioengineering and Biotechnology*, 8:604, 2020.
- [64] Metin Bicer, Andrew TM Phillips, Alessandro Melis, Alison H McGregor, and Luca Modenese. Generative deep learning applied to biomechanics: A new augmentation technique for motion capture datasets. *Journal of Biomechanics*, page 111301, 2022.
- [65] Alberto Leardini, Lorenzo Chiari, Ugo Della Croce, and Aurelio Cappozzo. Human movement analysis using stereophotogrammetry: Part 3. Soft tissue artifact assessment and compensation. *Gait & posture*, 21(2):212–225, 2005.
- [66] Lorenzo Chiari, Ugo Della Croce, Alberto Leardini, and Aurelio Cappozzo. Human movement analysis using stereophotogrammetry: Part 2: Instrumental errors. *Gait & posture*, 21(2):197–211, 2005.
- [67] Jennifer L Hicks, Thomas K Uchida, Ajay Seth, Apoorva Rajagopal, and Scott L Delp. Is my model good enough? Best practices for verification and validation of musculoskeletal models and simulations of movement. *Journal of Biomechanical Engineering*, 137(2), 2015.
- [68] Jack M Wang, Samuel R Hamner, Scott L Delp, and Vladlen Koltun. Optimizing locomotion controllers using biologically-based actuators and objectives. *ACM Transactions on Graphics (TOG)*, 31(4):1–11, 2012.
- [69] Ross H Miller, Brian R Umberger, Joseph Hamill, and Graham E Caldwell. Evaluation of the minimum energy hypothesis and other potential optimality criteria for human running. *Proceedings of the Royal Society B: Biological Sciences*, 279(1733):1498–1505, 2012.
- [70] Antonie J Van den Bogert, Thomas Geijtenbeek, Oshri Even-Zohar, Frans Steenbrink, and Elizabeth C Hardin. A real-time system for biomechanical analysis of human movement and muscle function. *Medical & Biological Engineering & Computing*, 51(10):1069–1077, 2013.
- [71] C Pizzolato, M Reggiani, L Modenese, and DG Lloyd. Real-time inverse kinematics and inverse dynamics for lower limb applications using OpenSim. *Computer Methods in Biomechanics and Biomedical Engineering*, 20(4):436–445, 2017.
- [72] Claudio Pizzolato, Monica Reggiani, David J Saxby, Elena Ceseracciu, Luca Modenese, and David G Lloyd. Biofeedback for gait retraining based on real-time estimation of tibiofemoral joint contact forces. *IEEE Transactions on Neural Systems and Rehabilitation Engineering*, 25(9):1612–1621, 2017.
- [73] T-W Lu and JJ O’connor. Bone position estimation from skin marker co-ordinates using Global Optimisation with joint constraints. *Journal of Biomechanics*, 32(2):129–134, 1999.

- [74] Emmanuel Roux, Stéphane Bouilland, A-P Godillon-Maquinghen, and Denis Bouttens. Evaluation of the Global Optimisation method within the upper limb kinematics analysis. *Journal of Biomechanics*, 35(9):1279–1283, 2002.
- [75] Sonia Duprey, Alexandre Naaim, Florent Moissenet, Mickaël Begon, and Laurence Chèze. Kinematic models of the upper limb joints for Multibody Kinematics Optimisation: An overview. *Journal of Biomechanics*, 62:87–94, 2017.
- [76] Morten Enemark Lund, Mark de Zee, Michael Skipper Andersen, and John Rasmussen. On validation of multibody musculoskeletal models. *Proceedings of the Institution of Mechanical Engineers, Part H: Journal of Engineering in Medicine*, 226(2):82–94, 2012.
- [77] David W Wagner, Vahagn Stepanyan, James M Shippen, Matthew S DeMers, Robin S Gibbons, Brian J Andrews, Graham H Creasey, and Gary S Beaupre. Consistency among musculoskeletal models: Caveat utilitor. *Annals of Biomedical Engineering*, 41(8):1787–1799, 2013.
- [78] Andrea Cereatti, Tecla Bonci, Massoud Akbarshahi, Kamiar Aminian, Arnaud Barré, Mickael Begon, Daniel L Benoit, Caecilia Charbonnier, Fabien Dal Maso, Silvia Fantozzi, et al. Standardization proposal of soft tissue artefact description for data sharing in human motion measurements. *Journal of biomechanics*, 62:5–13, 2017.
- [79] Benjamin J Fregly, Thor F Besier, David G Lloyd, Scott L Delp, Scott A Banks, Marcus G Pandy, and Darryl D D’lima. Grand challenge competition to predict in vivo knee loads. *Journal of Orthopaedic Research*, 30(4):503–513, 2012.
- [80] Allison L Kinney, Thor F Besier, Darryl D D’Lima, and Benjamin J Fregly. Update on grand challenge competition to predict in vivo knee loads. *Journal of Biomechanical Engineering*, 135(2), 2013.
- [81] P Westerhoff, F Graichen, A Bender, A Halder, A Beier, A Rohlmann, and G Bergmann. In vivo measurement of shoulder joint loads during activities of daily living. *Journal of Biomechanics*, 42(12):1840–1849, 2009.
- [82] A Asadi Nikooyan, HEJ Veeger, P Westerhoff, F Graichen, G Bergmann, and FCT Van der Helm. Validation of the Delft Shoulder and Elbow Model using in-vivo glenohumeral joint contact forces. *Journal of Biomechanics*, 43(15):3007–3014, 2010.
- [83] Sebastian Skals, Rúni Bláfoss, Michael Skipper Andersen, Mark de Zee, and Lars Louis Andersen. Manual material handling in the supermarket sector. Part 1: Joint angles and muscle activity of trapezius descendens and erector spinae longissimus. *Applied Ergonomics*, 92:103340, 2021.
- [84] Sebastian Skals, Rúni Bláfoss, Mark de Zee, Lars Louis Andersen, and Michael Skipper Andersen. Effects of load mass and position on the dynamic loading of the knees, shoulders and lumbar spine during lifting: A musculoskeletal modelling approach. *Applied Ergonomics*, 96:103491, 2021.
- [85] Giulia Bassani, Alessandro Filippeschi, and Carlo Alberto Avizzano. A dataset of human motion and muscular activities in manual material handling tasks for biomechanical and ergonomic analyses. *IEEE Sensors Journal*, 21(21):24731–24739, 2021.
- [86] Alexander Mathis, Steffen Schneider, Jessy Lauer, and Mackenzie Weygandt Mathis. A primer on motion capture with deep learning: Principles, pitfalls, and perspectives. *Neuron*, 108(1):44–65, 2020.
- [87] Runbei Cheng, Vikranth H. Nagaraja, Jeroen H. Bergmann, and Mark S. Thompson. Motion Capture Analysis & Plotting Assistant: An opensource framework to analyse inertial-sensor-based measurements. In *ISPO Trent International Prosthetics Symposium (TIPS) 2019*, pages 156–157, Manchester, United Kingdom, 2019. ISPO.
- [88] Runbei Cheng, Vikranth H. Nagaraja, Jeroen H. Bergmann, and Mark S. Thompson. An opensource framework to analyse marker-based and inertial-sensor-based measurements: Motion Capture Analysis & Plotting Assistant (MCAPA) 2.0. In *BioMedEng 2019*, London, United Kingdom, 2019.
- [89] Carnegie Mellon University – CMU Graphics Lab - Motion Capture Library. <http://mocap.cs.cmu.edu/>, 2003. (Accessed on 03/09/2022).
- [90] Dieter Büchler, Roberto Calandra, Bernhard Schölkopf, and Jan Peters. Control of musculoskeletal systems using learned dynamics models. *IEEE Robotics and Automation Letters*, 3(4):3161–3168, 2018.
- [91] Dorian Scholz, Stefan Kurowski, Katayon Radkhah, and Oskar von Stryk. Bio-inspired motion control of the musculoskeletal biobiped robot based on a learned inverse dynamics model. In *2011 11th IEEE-RAS International Conference on Humanoid Robots*, pages 395–400. IEEE, 2011.
- [92] Antonio Gonzales Marin, Mohammad S Shourijeh, Pavel E Galibarov, Michael Damsgaard, Lars Fritsch, and Freek Stulp. Optimizing contextual ergonomics models in human-robot interaction. In *2018 IEEE/RSJ International Conference on Intelligent Robots and Systems (IROS)*, pages 1–9. IEEE, 2018.

- [93] Marion Mundt, William R Johnson, Wolfgang Potthast, Bernd Markert, Ajmal Mian, and Jacqueline Alderson. A comparison of three neural network approaches for estimating joint angles and moments from Inertial Measurement Units. *Sensors*, 21(13):4535, 2021.

## 8 Supplementary Information

### 8.1 Neural Network performance

Output	<i>r</i>					NRMSE				
	Mean	SD	Max	Min	IQR	Mean	SD	Max	Min	IQR
<b>Subject-exposed</b>										
Joint angles	0.92	0.23	1.0	-0.07	0.03	0.25	0.2	0.79	0.04	0.28
Joint reaction forces	0.91	0.12	0.99	0.46	0.07	0.34	0.11	0.55	0.17	0.13
Joint moments	0.88	0.08	0.98	0.7	0.11	0.41	0.20	0.97	0.19	0.16
Muscle forces	0.84	0.30	0.99	0.07	0.08	0.37	0.17	0.69	0.10	0.18
Muscle activations	0.88	0.25	1.0	0.21	0.05	0.29	0.15	0.62	0.08	0.07
<b>Subject-naive</b>										
Joint angles	0.86	0.17	0.98	0.32	0.07	0.83	0.64	2.42	0.18	0.87
Joint reaction forces	0.77	0.31	0.98	-0.61	0.24	0.87	0.79	3.65	0.20	0.48
Joint moments	0.86	0.11	0.99	0.56	0.12	1.14	1.07	3.5	0.25	0.67
Muscle forces	0.94	0.04	0.97	0.85	0.01	0.49	0.53	1.86	0.09	0.28
Muscle activations	0.93	0.04	0.96	0.84	0.04	0.36	0.24	0.96	0.1	0.19

Table 3: Average Pearson’s Correlation Coefficient and Average NRMSE Values for Neural Network predictions compared with Musculoskeletal model outputs. Note: The average is taken over all output features and over all test trials (for a given output category). IQR refers to inter-quartile range.

Output	RMSE				
	Mean	SD	Max	Min	IQR
<b>Subject-exposed</b>					
Joint angles (in degrees)	2.91	1.86	8.24	1.07	1.48
Joint reaction forces (% Body Weight)	2.15	2.55	9.75	0.21	2.36
Joint moments (% Body Weight x Body Height)	0.02	0.02	0.06	0.0	0.02
Muscle forces (% Body Weight)	0.64	0.6	1.53	0.01	1.0
Muscle activations (%)	0.97	0.68	1.92	0.04	1.19
<b>Subject-naive</b>					
Joint angles (in degrees)	9.02	3.51	16.49	4.31	5.84
Joint reaction forces (% Body Weight)	5.08	6.02	26.57	0.28	6.08
Joint moments (% Body Weight x Body Height)	0.03	0.03	0.09	0.0	0.05
Muscle forces (% Body Weight)	0.42	0.4	1.38	0.06	0.4
Muscle activations (%)	1.0	0.66	2.03	0.14	1.08

Table 4: Average RMSE Values for Neural Network predictions compared with Musculoskeletal model outputs. Note: The average is taken over all output features and over all test trials (for a given output category). IQR refers to inter-quartile range.

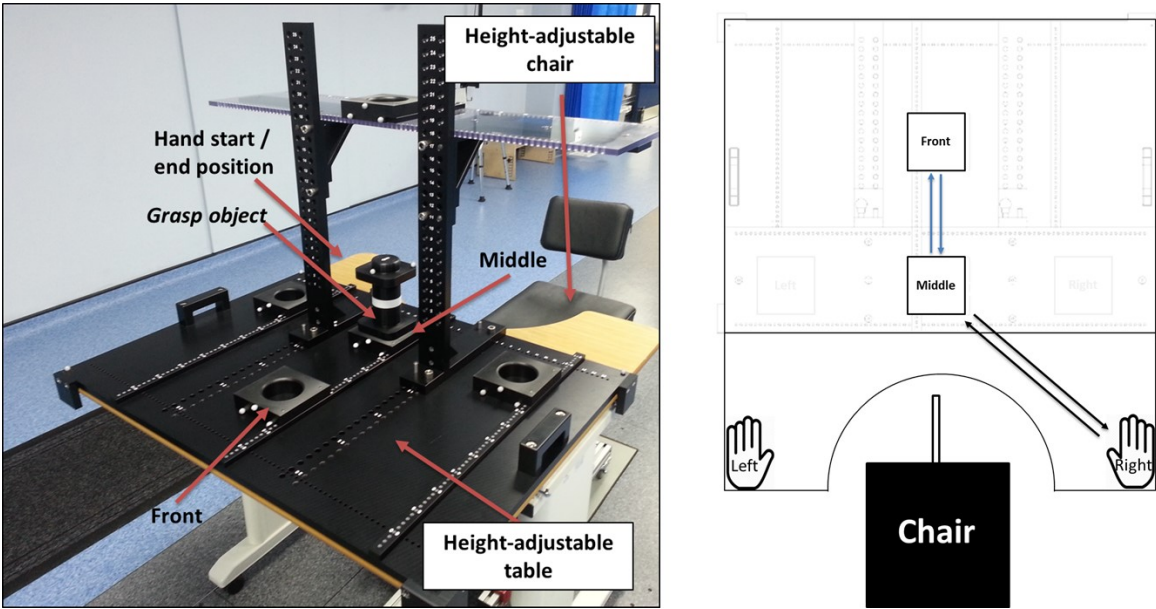


Figure 8: Left side: Custom-built apparatus for *Reach-to-Grasp* task execution in the Forward direction; Right-side: *Reach-to-Grasp* task setup.